Journal of Engineering and Sustainable Development
www.jeasd.org
Vol. 21, No.04, July 2017
ISSN 2520-0917

DESIGN AN OPTIMAL PID CONTROLLER WITH NONLINEAR FUNCTION USING BACTERIA FORAGING OPTIMIZATION FOR SINGLE FLEXIBLE LINK ROBOT MANIPULATOR

Dr. Ekhlas H. Karam[1], Noor S. Abdul-Jaleel[2], *Rokaia Sh. Habeeb[3]

1) Assist Prof., Computer Engineering Department, Al-Mustansiriyah University, Baghdad, Iraq.
2) Assist Lect., Electrical Engineering Department, Al-Mustansiriyah University, Baghdad, Iraq.
3) Assist Lect., Computer Engineering Department, Al-Mustansiriyah University, Baghdad, Iraq.

Abstract: This paper presents an optimal design of a modified Proportional Integral Derivative (PID) controller with nonlinear signum function for vibration control of a single-link flexible manipulator system. This manipulator is a Single Input Multi Output (SIMO) system with applied torque as the input signal, and the hub angle and tip deflection as the outputs. The dynamic model of the flexible link system is represented by finite element method. The Bacteria Foraging Optimization (BFO) algorithm is used to tune the parameters of the PID controller. A nonlinear signum function is added to improve the performance of this controller. Different types of inputs are tested with different payloads to illustrate the robustness of the control scheme. The scheme successfully reduces the effect of the vibration and minimize it to zero at the tip-end, even with payload variation.

Keywords: *single link flexible manipulator, PID controller, vibration control, bacterial foraging optimization.*

تصميم مسيطر PID امثل ذو دالة غير خطية بأستخدام طريقة BFO للسيطرة على ذراع روبوت مرن احادي الوصلة

الخلاصة: يقدم هذا البحث تصميم امثل لمسيطر PID معدل مع دالة Signum غير خطية للسيطرة على الاهتزازات في ذراع روبوت مرن أحادي الوصلة. نظام الذراع هو احادي الادخال و متعدد الاخراج، مع اعتبار العزم المسلط كقيمة ادخال وزاوية المحور واهتزاز نهاية الذراع كقيم اخراج. يتم تمثيل النموذج الديناميكي للذراع المرن احادي الوصلة باستخدام طريقة العناصر المحددة. يتم تنغيم مسيطر PID المعدل باستخدام طريقة BFO. تمت اضافة دالة Signum الغير خطية لغرض تحسين اداء المسيطر. التصميم المقترح تم فحصه لأكثر من اشارة ادخال و لأكثر من حمل و اظهرت النتائج تقليل الاهتزازات في نهاية الذراع المرن الى الصفر حتى مع تغيير الحمل.

1. Introduction

One of the modern industrial robots is the flexible robot manipulator system. This system has many advantages when compared to the rigid industrial robots, it has: lighter weight, higher payload to robot weight ratio, faster operation, less power consumption, and cheaper cost [1]. Difficulties in modelling arise due to the flexibility of the system, as it generates high vibration and oscillation at the tip-end [2]. The complexity of modelling is increased when a payload is carried by the flexible robot [3].

*Corresponding Author rokaia.shala@uomustansiriyah.edu.iq

In practice, the flexible robot is designed to achieve a single or multi task, such as taking up a payload, move to a specific location or track pre-planned trajectory and sets the payload. The payload variation has a significant impact on the dynamic behavior of the flexible robot [4]. Therefore, an accurate modelling of flexible link manipulator is required to represent the dynamic characteristics and the actual behavior of the system.

Modelling of a single Flexible Link Manipulator (FLM) has been widely evaluated in the literature. The FLM robotic systems are continuous dynamical nonlinear systems, which are described by ordinary and partial differential equations with an infinite number of degrees of freedom. Practically, the exact solution of these systems is not feasible and the infinite dimensional model establishes severe constraints on the design of controllers Therefore, the dynamic equations are discretized most commonly using the Assumed Modes Method (AMM), the Finite Element Method (FEM) or the lumped parameter method. The FEM and AMM use either the Lagrangian formulation or the Newton–Euler recursive formulation [5].

The AMM assumes that the flexibility of link is ordinary represented by truncated finite model series in terms of spatial mode Eigen functions, with time-dependent mode amplitudes. The difficulty in finding methods for single links with irregular cross sections and multi-link manipulators is the main obstacle of the AMM [6].

Many boundary conditions must be considered for solving the major set of differential equations derived in the FEM. However, in most cases, these conditions are uncertain for flexible links [7].

When deriving a closed-form of the dynamic equations of motion for the flexible links, the first several modes in AMM are kept by assumption, while the higher modes are disregarded. The simplest method for analysis is the lumped parameter model. Unlike the spring and mass system, in which the manipulator does not produce accurate results [6].

Different control approaches have been applied to solve the problems of vibration and tip deflection of flexible manipulator systems. Two main cases cause problems in the FLMs controller design, the first is the high order of the system. The second is the non-minimum phase dynamics of the system, which exist between the applied input torque and the tip position at the hub joint of the system [1].

Various methods have been suggested in the literature to control the FLMs, some of these are:

Linear control methods such as conventional PID control [8], linear quadratic regulator [9], generalized proportional integral control [10], pole placement control [11], integral resonant control [1], H-infinity [12]. Modified linear controllers such as PID tuned by Particle Swarm Optimization (PSO) algorithm [13], PSO for vibration funnel of flexible manipulator structures [14], and proportional derivative controller tuned by cuckoo search [15].

Nonlinear control methods such as: nonlinear feedback [16], optimal nonlinear feedback [17], fuzzy logic control technique [2, 11], neural network control technique [18], neuro-fuzzy control [19]. Hybrid linear/nonlinear control methods such as: modified PID [20], neural network for tuning modified PID [21].

Generally, due to the nonlinear dynamic structure of the flexible manipulator, it is difficult to be accurately controlled by linear control method [22]. In this paper, the characteristic of the mathematical model of single FLM is investigated. The FEM is used for the dynamic modelling of the system.

The transfer function of this system is SIMO. BFO is used to tune the PID parameters to improve the performance of the controller due to its encouraging results shown in prior work such as [23] which gives a clear comparison between three optimization algorithms in tuning PID control. [24, 25]. An optimal modified PID controller with nonlinear signum function is designed for the vibration control of the single FLM.

The rest of this paper is organized as follow. Section 2 describes the mathematical model of the single FLM. In Section 3 the proposed controller of the flexible manipulator is illustrated. Different simulation results are presented in Section 4. Finally, the summary and conclusions of the overall work is addressed in Section 5.

2. Mathematical Model of Single FLM

This section provides a brief description for the dynamic model of the FLM, which is developed by using the FEM and infinite-dimensional transfer function.

2.1. *Modelling the Single FLM Using FEM*

The schematic diagram of the single FLM which is used in this work is shown in Fig. 1. The symbols pointed on this figure are described by Table 1 along with the Sheffield FLM physical parameters that is considered in this study [26].

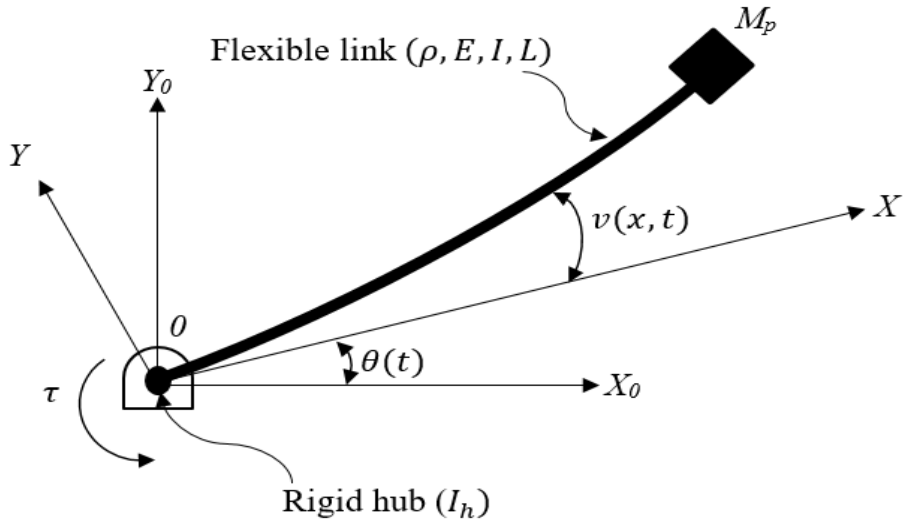

Figure 1. Schematic diagram of the FLM.

Table 1. Parameters of an FLM.

Symbol	Parameter Description	Sheffield FLM Physical Parameters
XOY	The moving coordinate frame.	
X_0OY_0	The stationary coordinate frame.	
E	The Young Modulus.	$71*10^9$ N/m^2
I	The second moment of inertia.	$5.1924 * 10^{-11}$ m^4
ρ	The mass density per unit length of the FLM.	2710 kg/m^3
l	The length of flexible beam.	900 mm
A	Cross-sectional area.	$6.08332*10^{-2}$ m^2
I_h	The Hub inertia.	$5.8598 * 10^{-4}$ kgm^2
τ	The input torque applied at the hub by a motor.	
θ(t)	The angular displacement (hub-angle) of the manipulator.	
w(x, t)	The elastic deflection of a point along the manipulator, at a distance x from the hub of the manipulator.	
M_p	The payload mass attached at the end-point of link.	

Both *XOY* and X_0OY_0 axes lie in a horizontal plane and all rotation occurs about a vertical axis, thus allowing the manipulator to vibrate dominantly in the horizontal direction and hence, the gravity effects are neglected. In addition, the flexible link is considered to have constant cross section and unified material properties [26].

The overall displacement $y(x,t)$ of a point along the FLM from the hub at a distance x can be defined as [15, 26]:

$$y(x,t) = x\theta(t) + w(x,t) \quad (1)$$

The FEM is used to solve the dynamic problems that resulting in:

$$w(x,t) = N_a(x)Q_a(t) \quad (2)$$

Where $N_a(x)$ is the shape function and $Q_a(t)$ is the nodal displacement. The displacement $y(x,t)$ can be represented as:

$$y(x,t) = N(x)Q_b(t) \quad (3)$$

Where $N(x) = [x \;\; N_a(x)]$ and $Q_b(t) = [\theta(t) \;\; Q_a(t)]^T$

The distance x and the angle $\theta(t)$ are global variables, while $Q_a(t)$ and $N_a(x)$ are local variables. Defining $k = x - \sum_{i-1}^{n-1} l_i$ as a local variable of the n^{th} element, where l_i is the length of the i^{th} element, and using Macsyma, the shape function can be represented by [26].

$$N(k) = \left[k + l(n-1)\ \ 1 - \frac{3k^2}{l^2} + \frac{2k^3}{l^3}\ \ \ k - \frac{2k^2}{l} + \frac{k^3}{l^2}\ \ \frac{3k^2}{l^2} - \frac{2k^3}{l^3}\ \ - \frac{k^2}{l} + \frac{k^3}{l^2}\right]$$

$$\varphi = \frac{d^2N(k)}{dk^2} = \left[0\ \ \frac{12k}{l^3} - \frac{6}{l^2}\ \ \frac{6k}{l^2} - \frac{4}{l}\ \ \frac{6}{l^2} - \frac{12k}{l^3}\ \ \frac{6k}{l^2} - \frac{2}{l}\right]$$

The element stiffness K_n and element mass M_n matrices can be defined as [26]:

$$K_n = \int_0^l EI(\varphi^T \varphi)dk \qquad (4)$$

$$M_n = \int_0^l \rho A(N^T N)dk \qquad (5)$$

By solving (4) and (5) for *n* elements, the element stiffness and element mass matrices can be obtained as [26]:

$$K_n = \frac{EI}{l^3}\begin{bmatrix} 0 & 0 & 0 & 0 & 0 \\ 0 & 12 & 6l & -12 & 6l \\ 0 & 6l & 4l & -6l & 4l \\ 0 & -12 & -6l & 12 & -6l \\ 0 & 6l & 2l & -6l & 4l \end{bmatrix}$$

$$M_n = \frac{\rho Al}{420}\begin{bmatrix} 140l^2(3n^2-3n+1) & 21l(10n-7) & 7l^2(5n-3) & 21l(10n-3) & -7l^2(5n-2) \\ 21l(10n-7) & 156 & 22l & 54 & -13l \\ 7l^2(5n-3) & 22l & 4l & 13l & -3l^2 \\ 21l(10n-3) & 54 & 13l & 156 & -22l \\ -7l^2(5n-2) & -13l & -3l^2 & -22l & 4l^2 \end{bmatrix}$$

Assembling the above matrices and utilizing the Euler-Lagrange equation of motion, the dynamic equation of the FLM can be represented by [26]:

$$M\ddot{Q}(t) + KQ(t) = F(t) \qquad (6)$$

Where *K* and *M* are the stiffness and global mass matrices respectively, the K_n and M_n are assembled to obtain these matrices. While, *F*(*t*) is the vector of external torques and $Q(t)=[\theta\ w_0\ \theta_0\ \ldots\ w_\alpha\ \theta_\alpha]^T$, where θ, $\theta_\alpha$and w_α refer to the hub-angle output, rotation of the manipulator and end-point deflection respectively [26]. With $n = 1$, the elements of *M*, *K*, *F*(*t*), and *Q*(*t*) become:

$$M = \frac{\rho Al}{420}\begin{bmatrix} 140l^2 & 63l & 14l^2 & 147l & -21l^2 \\ 63l & 156 & 22l & 54 & -13l \\ 14l^2 & 22l & 4l^2 & 13l & -3l^2 \\ 147l & 54 & 13l & 156 & -22l \\ -21l^2 & -13l & -3l^2 & -22l & 4l^2 \end{bmatrix}$$

$$K = \frac{EI}{l^3}\begin{bmatrix} 0 & 0 & 0 & 0 & 0 \\ 0 & 12 & 4l^2 & -12 & 6l \\ 0 & 6l & -6l & -6l & 2l^2 \\ 0 & -12 & 13l & 12 & -6l \\ 0 & 6l & 2l^2 & -6l & 4l^2 \end{bmatrix}$$

$$F(t) = [\tau \ 0 \ 0 \ 0 \ 0 \ 0]^T$$

$$Q(t) = [\theta \ w_0 \ \theta_0 \ w_\alpha \ \theta_\alpha]^T$$

By consolidating the payload and the hub inertia into the model of the system, a new system mass matrix that consolidates the hub inertia and the payload can be determined as:

$$M = \frac{\rho Al}{420}\begin{bmatrix} 140l + l\ Mp + Ih & 63l & 14l & 147l + IMp & -21l \\ 63l & 156 & 22l & 54 & -13l \\ 14l & 22l & 4l & 13l & -3l \\ 147l + IMp & 54 & 13l & 156 + Mp & -22l \\ -21l & -13l & -3l & -22l & 4l \end{bmatrix}$$

Here, $Q(0)$ is assumed to be zero. By combining the initial conditions and considering flexural and angular displacements at the hub as zero, the second and third rows and columns in K, M, Q and F can be ignored [26]. These yield to:

$$K = \frac{EI}{l^3}\begin{bmatrix} 0 & 0 & 0 \\ 0 & 12 & -6l \\ 0 & -6l & 4l^2 \end{bmatrix}$$

$$M = \frac{\rho Al}{420}\begin{bmatrix} 140\ l^2 + l^2 M_p + I_h & 147l + lM_p & -21l^2 \\ 147l + lM_p & 156 + M_p & -22l \\ -21l^2 & -22l & 4l^2 \end{bmatrix}$$

$$Q(t) = [\theta \ w_\propto \ \theta_\propto]^T \quad \text{and} \quad F(t) = [\tau \ 0 \ 0]^T$$

2.2. *State Space and Transfer Functions Representation*

The state space form of the dynamic equation of the flexible manipulator (6) is represented by:

$$\dot{v} = Av + Bu \tag{7}$$

$$y = Cv + Du$$

Where

$$A = \begin{bmatrix} 0_3 & I_3 \\ -M^{-1}K & 0_3 \end{bmatrix},\ B = \begin{bmatrix} 0_{3\times1} \\ M_1^{-1} \end{bmatrix},\quad D = 0_{3\times1}$$

And

$$u = \tau$$

$$v = \left[\theta \;\; w_{\propto} \;\; \vartheta_{\propto} \;\; \dot{\theta} \;\; \dot{w}_{\propto} \;\; \dot{\theta}_{\propto}\right]^{T}$$

0_3 is a 3 × 3 null matrix, I_3 is a 3×3 identity matrix, $0_{3\times1}$ is a 3 × 1 null vector and M_1^{-1} is the first column of M^{-1}. The output matrix C depends on the desired transfer functions. Considering C=[1 0 0 0 0 0] for the torque input to hub-angle output, while C=[L 1 0 0 0 0] for torque input to end-point displacement [15, 26].
The transfer functions from torque input to both hub-angle output of the manipulator and end-point displacement can be obtained as [26]:

$$G_1(s) = \frac{30\propto^2 l^7 s^4 - 48600\propto\beta l^4 s^2 + 4536000\beta^2 l}{s^2\begin{bmatrix}\left((15\propto^2 l^8 + 3600\propto l^6 I_h)M_p + \propto^3 l^8 + 300\propto^2 l^6 I_h\right)s^4 \\ +\left((39600\propto\beta l^5 + 1512000\beta l^3 I_h)M_p + 5220\propto^2\beta l^5 + 367200\propto\beta l^3 I_h\right)s^2 \\ +\left(4536000\beta^2 l^2 M_p + 1512000\alpha\beta^2 l^2 + 4536000\beta^2 I_h\right)\end{bmatrix}} \quad (8)$$

$$G_2(s) = \frac{(3600\alpha l^6 M_p + 300\propto^2 l^6)s^4 + (1512000\beta l^3 M_p + 367200\alpha\beta l^3)s^2 + 4536000\beta^2}{s^2\begin{bmatrix}\left((15\propto^2 l^8 + 3600\propto l^6 I_h)M_p + \propto^3 l^8 + 300\propto^2 l^6 I_h\right)s^4 \\ +\left((39600\propto\beta l^5 + 1512000\beta l^3 I_h)M_p + 5220\propto^2\beta l^5 + 367200\propto\beta l^3 I_h\right)s^2 \\ +\left(4536000\beta^2 l^2 M_p + 1512000\alpha\beta^2 l^2 + 4536000\beta^2 I_h\right)\end{bmatrix}} \quad (9)$$

Where α=ρAl represents the weight and β=EI represents the flexural stiffness of the manipulator [26]. The Sheffield FLM as presented in [26] is considered in this study with the physical parameters shown in Table 1.
Equations 8 and 9 can be written as:

$$G_{1b}(s) = \frac{(283.86M_P + 3.51)s^4 + (4116760M_P + 148339.8)s^2 + 6.33\times10^7}{(0.3M_P + 0.0035)s^6 + (1537.2M_P + 340.36)s^4 + (5.13\times10^7 M_P + 257860)s^2} \quad (10)$$

$$G_{2b}(s) = \frac{0.32s^4 - 17669.9s^2 + 5.69\times10^7}{(0.3M_P + 0.0035)s^6 + (1537.2M_P + 340.36)s^4 + (5.13\times10^7 M_P + 257860)s^2} \quad (11)$$

Both $G_{2b}(s)$ and $G_{1b}(s)$ has six poles, two are at the origin, for $M_p \geq 0$, two of the four poles are negative, and the remaining are imaginary poles. These poles cause system vibration. Since, all zeros of the transfer function $G_{1b}(s)$ for $M_p \geq 0$ lies on the imaginary axis, therefore this transfer function result in minimum phase manner. While the zeros of $G_{2b}(s)$ lead to a non-minimum phase [26].

3. Tuning PID Controller Using BFO

PID controllers have been used in wide range of applications, because of their simple design, low cost and effectiveness [27]. These controllers have three parameters that are illustrated in terms of time, where P depends on the present error, I depends on the

accumulation of past errors and *D* is a prediction of future errors based on current rate of change [27], these terms of parameters are summed to calculate the output of the PID controller and minimize the error by regulating the process control inputs. The controller output can be defined by $u(t)$ as:

$$u(t) = K_p\, e(t) + K_i \int_0^t e(t)dt + K_d \frac{d\, e(t)}{d(t)} \qquad (12)$$

Where K_p is the proportional gain, K_i is the integral gain, K_d is the derivative gain, $e(t)$ is the error as a function of time. Many tuning methods have been suggested to determine the suitable values for the PID controller parameters (K_p, K_i, and K_d), one of these methods is the BFO. The BFO is an algorithm that is based on the behavior of food searching of E. coli bacteria [27]. This algorithm is divided into four stages:

1. Chemotaxis.
2. Swarming.
3. Reproduction.
4. Elimination dispersal.

3.1. Chemotaxis

The movement of bacteria when searching for food passes through two stages: swimming and tumbling. The combination of these stages is called chemotaxis [27]. In this stage, the movement of bacteria alternates between swimming when the bacteria move in the same direction, and tumbling when the bacteria move in different direction [28].

3.2. Swarming

The swarm stage can be illustrated as the behavior of bacteria that move together in groups looking for the best location of food, and sending attraction signals to other bacteria to reach the best location, so that they always do movements in a high density [27].

Assume $\theta^j(i,k,l)$ represents j^{th} bacteria, i^{th} chemotactic, k^{th} reproductive and l^{th} elimination stage. The function of the swarm can be represented as [29]:

$$J_{ss} = \left(\theta, P(i,k,l)\right) = \sum_{j=1}^{c} J_{ss}^{j}\left(\theta, \theta^j(i,k,l)\right) =$$

$$\sum_{j=1}^{c}\left[-D_{att}\, exp\left(W_{att}\sum_{n=1}^{m}(\theta_n - \theta_n^i)^2\right)\right] + \sum_{j=1}^{c}\left[H_{rep}\, exp\left(W_{rep}\sum_{n=1}^{m}(\theta_n - \theta_n^i)^2\right)\right] \qquad (13)$$

Where, c is the total number of bacteria, m represents the number of parameters to be optimized, D_{att} is the attractant's depth which is released by the bacteria, W_{att} is width of the attractant signal, H_{rep} is height of the repellent effect magnitude, and W_{rep} is width of the repellent signal [30].

3.3. Reproduction

In the process of reproduction the healthier bacteria with good foraging result divided into two bacteria, they replace the least healthy bacteria which die, and keep the population of the bacteria constant [29].

3.4. Elimination Dispersal

The sudden changes in the environment may happen where bacteria live due to many reasons. In this stage the bacteria are selected randomly to be exchanged by new bacteria located at a new random place within the optimization domain. Then, the bacteria are dispersed till finding the more productive areas nearer to the food location [30]. The flowchart that explain the BFO algorithm is shown in Figure 2, where *Ns* is the swimming step, *Nre* is the number of reproduction steps, *Nc* is the number of chemotaxis steps and *Ned* is the number of elimination dispers

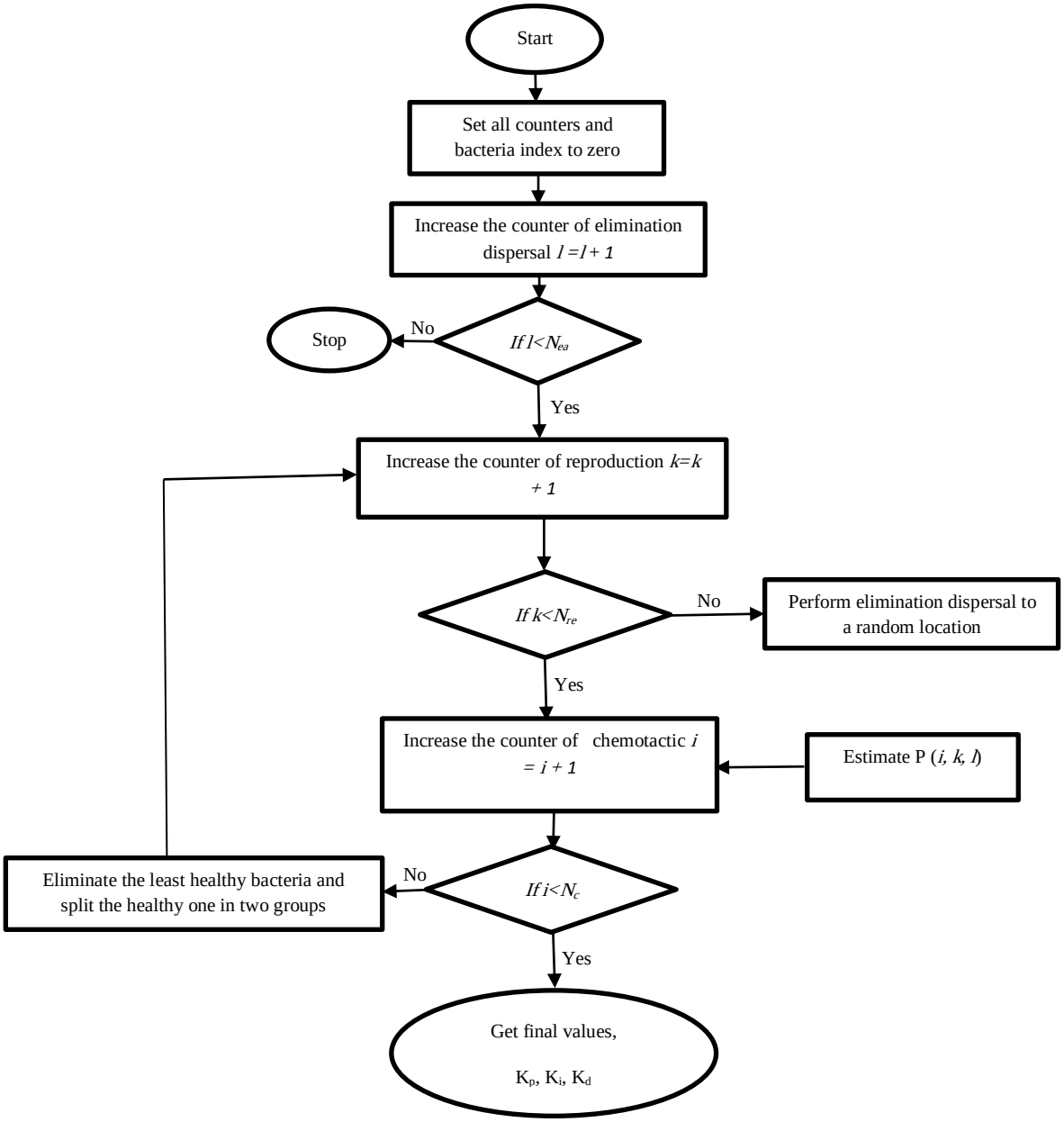

Figure 2. The flowchart of BFO algorithm.

4. The Complete Controller Scheme

The block diagram for the proposed controller is shown in Fig. 3. Instead of using standard PID, a modified PID (PI-D) is used in order to avoid the derivative kick when a sudden change occur in the input signal.

The modified PID parameters K_p, K_i *and* K_d are the same optimized parameters obtained when the traditional PID is connected.

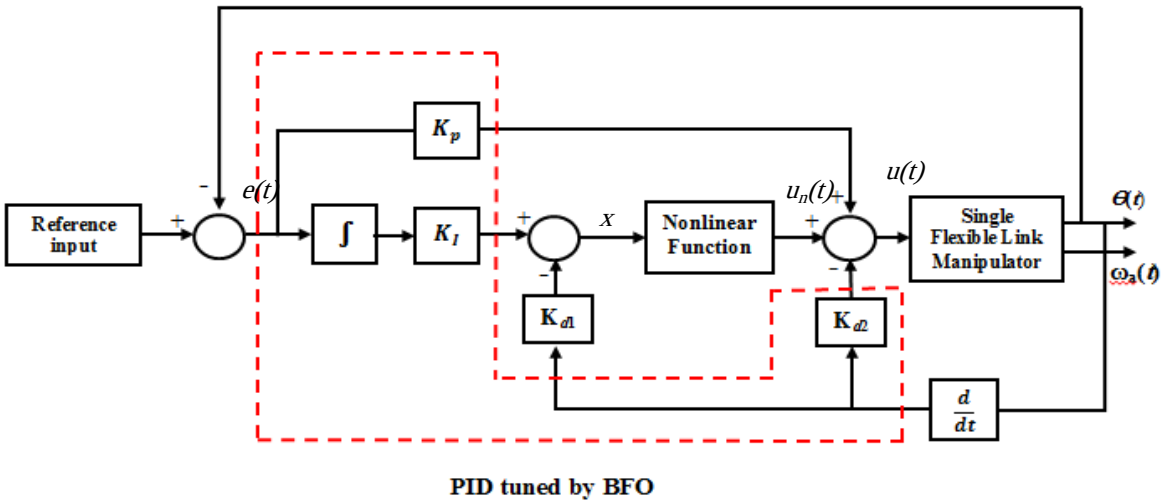

Figure 3. The block diagram for the overall controlled system.

This figure shows that the control signal $u(t)$ have the following equation:

$$u(t) = K_p\, e(t) + u_n(t) - K_{d2}\frac{d\theta}{dt} \qquad (14)$$

Where $u_n(t)$ is the output of the nonlinear function that is given by:

$$u_n(t) = sign\,(K_n x) * \sqrt{x^3} \qquad (15)$$

$$x = K_i \int_0^t e(t)dt - K_{d1}\frac{d\theta}{dt} \qquad (16)$$

Where K_n and K_{d1} are suitably selected gains, the parameters of (K_p, K_i, and K_{d2}) are determined by the BFO algorithm.

5. Simulation Results and Discussion

The complete Matlab Simulink connection of the proposed controller for the single FLM with mode n=1 is illustrated in Fig. 4.

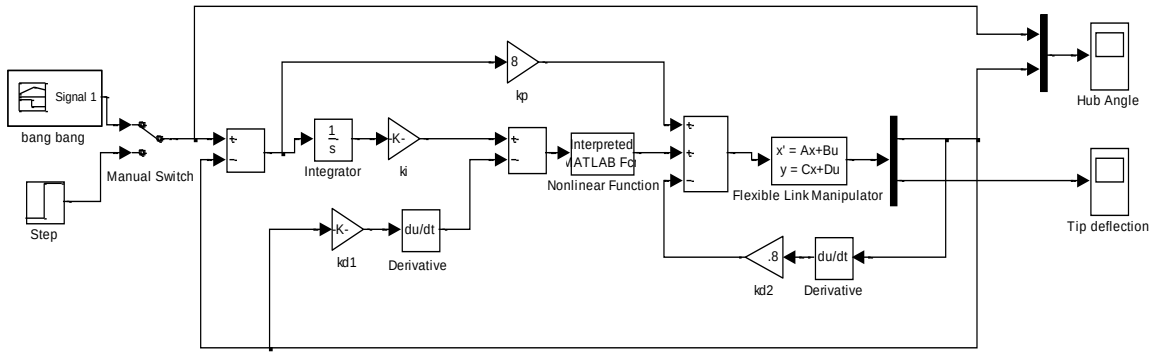

Figure 4. Matlab Simulink for the overall controlled system.

The parameters of BFO algorithm shown in Table 2 are declared in sections 3.2 and 3.4.

Table 2. BFO parameters used in tuning the PID controller

The parameters of BFO algorithm	Values
c	10
N_s	2
N_{re}	4
N_c	10
N_{ed}	2
H_{rep}	0.1
W_{rep}	10
W_{att}	0.04
D_{att}	0.01

The performance index considered in this paper to tune the modified PID parameters is the Integral Absolute Error (IAE). The tuned parameters of the controller scheme are (K_p=8, K_i=0.01, K_{d1}=0.05, K_{d2}=0.8, and K_n=0.8), in order to show the efficiency of the proposed controller, different cases are investigated:

5.1. Simulation for Fixed Payload

The unit step response for the single FLM controlled by modified PID controller, with/without the nonlinear function $u_n(t)$, with a load of 20g for the hub angle and the tip deflection, are shown in Fig. 5.

The results when only PID controller is used show that the hub angle tracks the desire hub angle of the system with a steady state error of 0.0001, rise time of 0.237 second and 6.02 percentage overshoot.

The system with PID and the nonlinear function result in zero steady state error, rise time of 0.227 second, and 8.11 percentage overshoot. Similarly, Fig. 5 (b) shows the result of the tip deflection, which has been regulated close to zero deflection with a maximum peak to peak deflection of 17.4 for PID only and with deflection of 17.8 for PID and the nonlinear function.

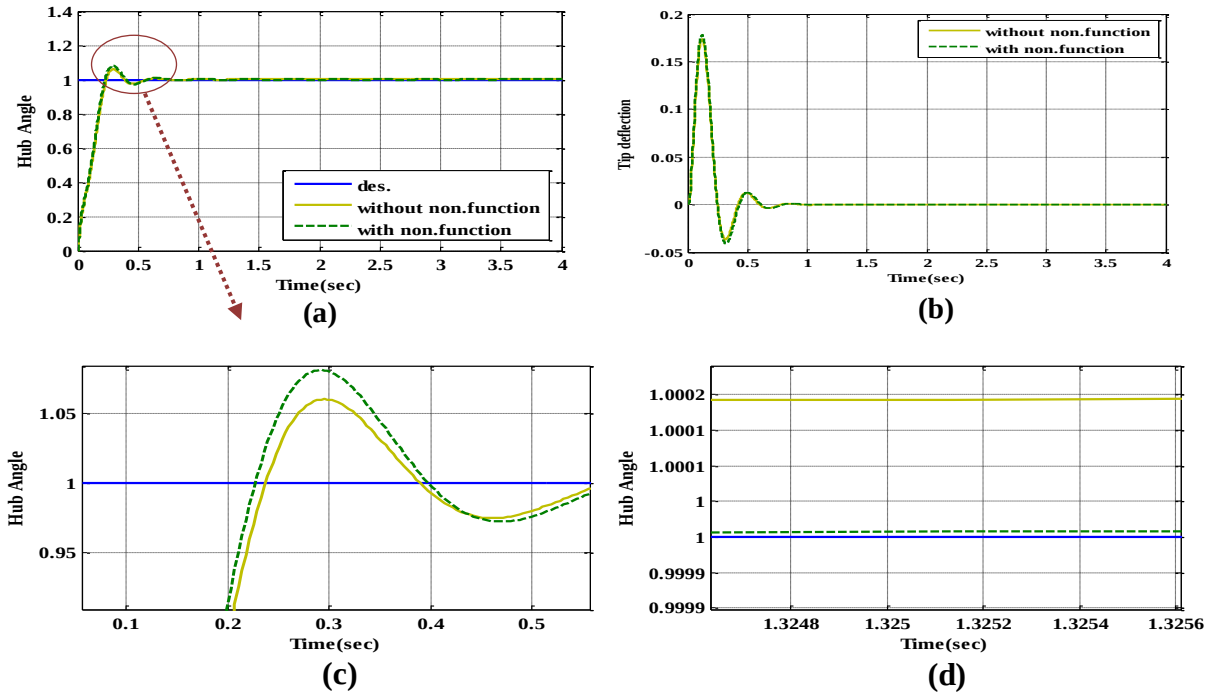

Figure 5. Unit step response with/without the nonlinear function for (a) hub angle, (b) tip deflection, (c) transient for the hub angle, (d) the steady state for hub angle.

5.2 Simulation with Different Payloads

The performance of the single FLM with the proposed controller tested also with different values of payload. Fig. 6 shows the hub angle, tip deflection, error, and control signal with payload values of 20g, 30g and 50g for a unit step input.

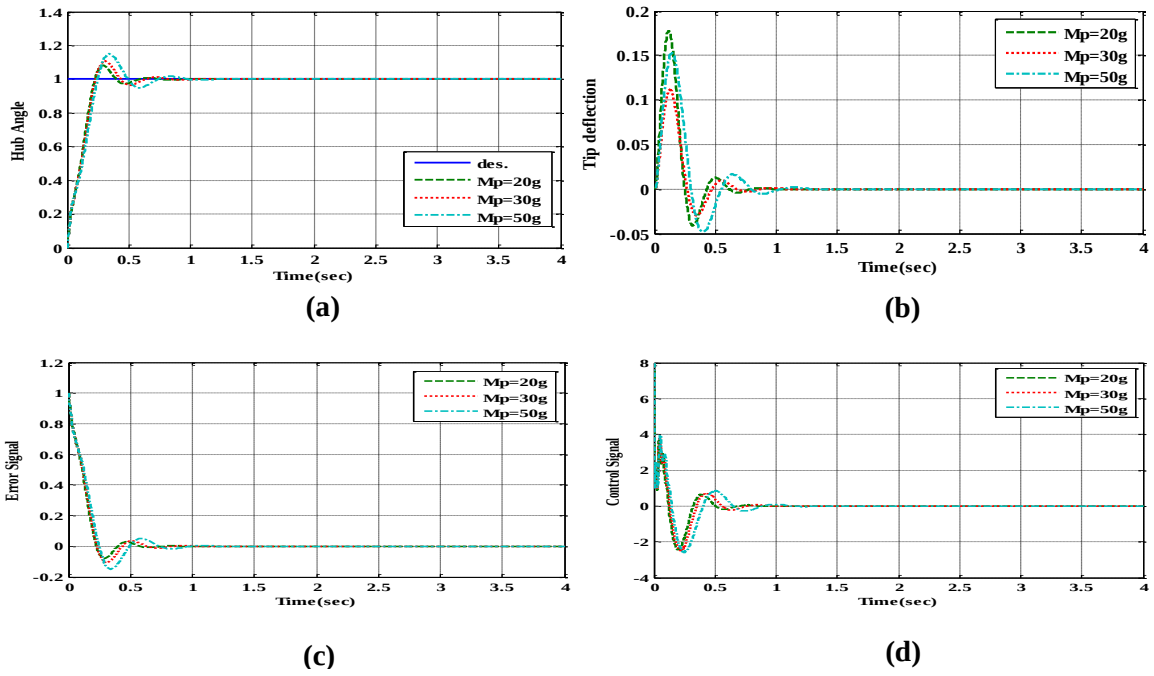

Figure 6: Unit step response with different loads (20, 30, and 50 gram) for:
(a) Hub angle, (b) Tip deflection, (c) Error signal, (d) Control signal.

Table 3. Summary of the simulation results with different payload values.

Payload	Hub angle Maximum percentage overshoot %	Hub angle steady state error	Hub angle Rise time	Hub angle Settling time	Tip deflection maximum percentage peak to peak deflection %
20	8.11	0	0.227	0.516	17.79
30	10.75	0	0.233	0.581	11.2
50	14.91	0	0.247	0.690	15.33

These results show that the maximum overshoot of the hub angle, maximum tip deflection, rise time, and settling time change with different payload values. Table 3 summarizes the time response specifications of the hub angle and the tip deflection with different payload values.

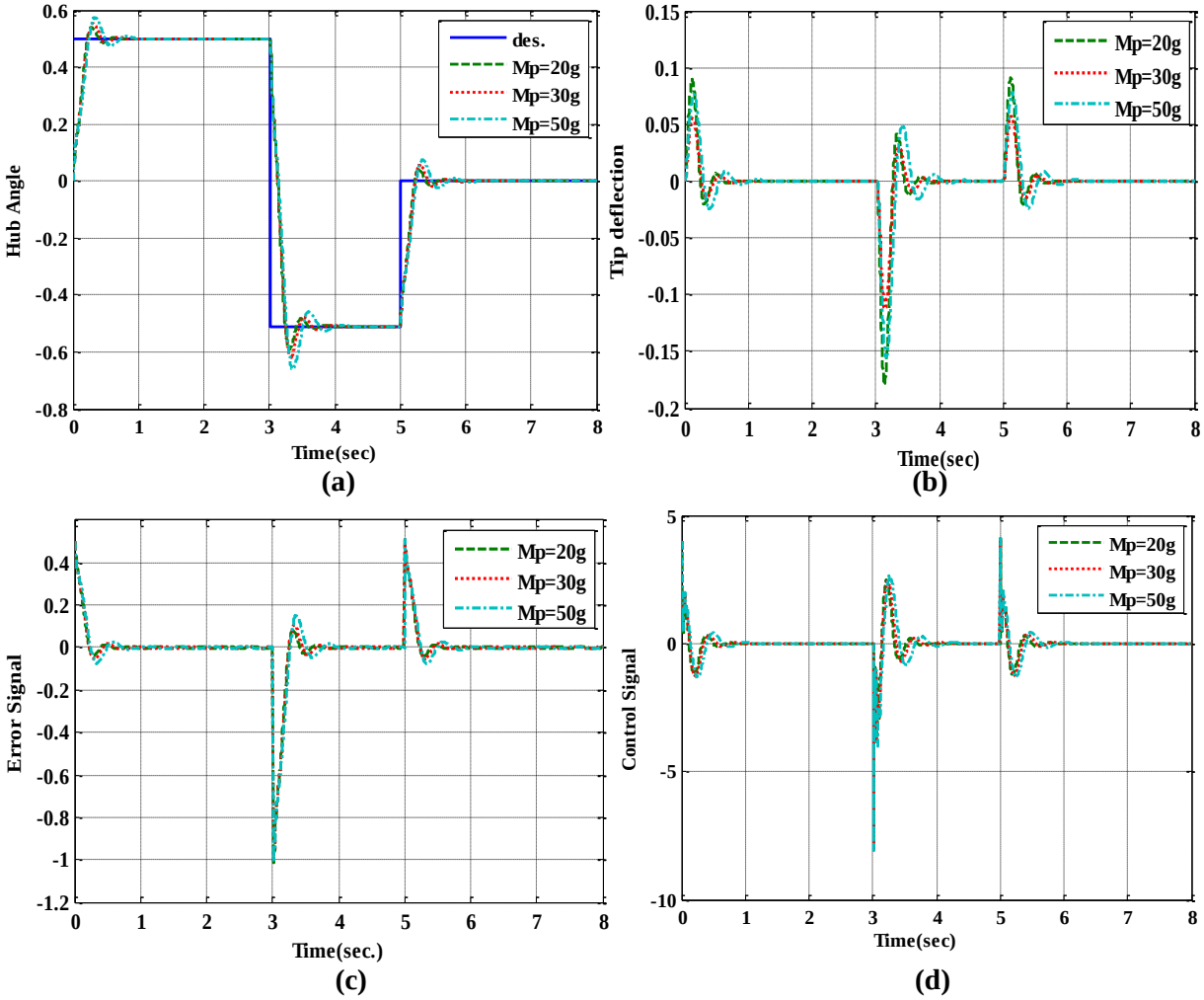

Figure 7. Bang-bang input response with different loads (20, 30, and 50 gram) for:
(a) Hub angle, (b) Tip deflection, (c): Error signal, (d) Control signal.

The results in Table 3 imply that as the payload increases, the system exhibits higher settling time, rise time and overshoot. While the peak to peak deflection decreases when the payload increases. The results of the hub angle and the tip deflection demonstrate the capability of the proposed controller when the payload is changed.

Fig. 7 shows the hub angle, tip deflection, error, and control signal with different payload values for bang-bang input. The error and control signal show that the derivative kick does not occur during a sudden change in the input signal.

6. Summary and Conclusions

In this paper, an optimal PID controller which parameters are tuned by BFO method with signum function has been designed for the single FLM modelled by the FE method. The signum function is used to enhance the performance of the PID controller. The input of the signum function is the sum of the integral error and the derivative of the hub angle, the output of this function is summed with the output of the PD controller to perform the control signal for the single FLM. The proposed controller scheme suppresses the vibration and achieves accurate tracking performance. The robustness and tracking performance with payload variation were investigated using Matlab Simulink simulation.

7. References

1. Pereira, E., et al. (2011). "Integral Resonant Control for Vibration Damping and Precise Tip-Positioning of a Single-Link Flexible Manipulator", Mechatronics, IEEE/ASME, Vol. 16, Issue 2, pp. 232-240.
2. Auwalu M. Abdullahi, Z. Mohamed and Mustapha Muhammad (2013). "A PD-Type Fuzzy Logic Control Approach for Vibration Control of a Single-Link Flexible Manipulator", International Journal of Research in Engineering and Science (IJRES), ISSN (Online): 2320-9364, ISSN (Print): 2320-9356, Vol. 1, Issue 4, pp. 37-47.
3. Martins J.M., Mohammed Z., Tokhi M.O., Sa'da Costa J.and Botto M.A. (2003). "Approaches for dynamic modeling of flexible manipulator systems", Control Theory and Applications, IEE Proceedings, Vol. 150, Issue 4, pp. 401-411.
4. Tokhi MO, Mohamed Z, Shaheed MH (2001). "Dynamic Characterization of a Flexible Manipulator System", Robotica, Vol. 19, Issue 5, pp. 571-580.
5. Santosha Kumar Dwivedy a, Peter Eberhard (2006). "Dynamic Analysis of Flexible Manipulators, a literature review", Mechanism and Machine Theory, Vol. 41, Issue 7, pp. 749–777.
6. R.J. Theodore, A. Ghosal (1995). "Comparison of the Assumed Modes and Finite Element Models for Flexible Multilink Manipulators", the International Journal of Robotics Research, Vol. 14 (2), pp. 91–111.
7. G.G. Hastings, W.J. Book (1986). "Verification of a Linear Dynamic Model for Flexible Robotic Manipulators", Proceedings of the IEEE International Conference on Robotics and Automation, Vol. 3, pp. 1024–1029.
8. Dinesh Singh Rana, Deepika (2014). "Modelling, Stability Analysis and Control of Flexible Single Link Robotic Manipulator", International Journal of Advanced Research in Electrical, Electronics and Instrumentation Engineering, ISSN (Print): 2320–3765, ISSN (Online): 2278–8875, Vol. 3, Issue 2.

9. Ramesh Gamasu (2014). "Pre-Load Torque Responses for Flexibility in Single Link Manipulator", International Journal of Hybrid Information Technology, ISSN: 1738-9968, Vol. 7, No. 2, pp. 103-112, 2014.
10. J. Becedas, V. Feliu and H. Sira-Ramrez (2007). "GPI Control for a Single-Link Flexible Manipulator", Proceedings of the World Congress on Engineering and Computer Science, San Francisco, USA, October 24-26.
11. Auwalu M. Abdullahi, Z. Mohamed, Mustapha Muhammad, AA Bature (2013). "Vibration Control Comparison of a Single Link Flexible Manipulator Between Fuzzy Logic Control and Pole Placement Control", International Journal of Scientific and Technology Research, ISSN 2277-8616, Vol. 2, Issue 12.
12. Roberd Saragih and Dede Tarwidi (2012). "Vibration Reduction on Single Flexible Manipulator using H_∞ Control", Journal of the Indonesian Mathematical Society**.**
13. Hanim Mohd Yatim and Intan Z. Mat Daru (2013). "Swarm Optimization of an Active Vibration Controller for Flexible Manipulator", Latest Trends in Circuits, Control and Signal Processing, Malaysia, ISBN: 978-1-61804-173-9, pp. 139-146.
14. Hanim Mohd Yatim and Intan Z. Mat Darus (2014). "Self-Tuning Active Vibration Controller Using Particle Swarm Optimization for flexible manipulator system", Wseas Transactions on Systems and Control Malaysia, E-ISSN: 2224-2856, Vol. 9.
15. Ali Abdulhussain Al-Khafaji, Intan Z. Mat Darus (2014). " Controller Optimization using Cuckoo Search Algorithm of a Flexible Single-Link Manipulator", First International Conference on Systems Informatics, Modelling and Simulation, IEEE Computer Society, pp. 31-36.
16. S. S. Ge, T. H. Lee, and G. Zhu (1997). "A Nonlinear Feedback Controller for a Single-Link Flexible Manipulator Based on a Finite Element Model", Journal of Robotic Systems 14(3), pp. 165–178.
17. Masoud Taleb Ziabari, Ali Reza Sahab and Valiallah Afsar (2013). "Stability In a Flexible Manipulator Using Optimal Non Linear Controller", Journal of Basic and Applied Scientific Research, ISSN: 2090-4304, pp. 323-329.
18. Tang, Sun F., Sun Z. (2006). "Neural Network Control of Flexible-Link Manipulators Using Sliding Mode", Neuro computing, n0. 70, pp. 288-295,.
19. S. Mallikarjunaiah and S. Narayana Reddy (2013). "Adaptive Neuro-Fuzzy Interface System Controller for Flexible Link Manipulator", Mediamira Science Publisher, Vol. 54, No. 2.
20. Tamer Mansour, Atsushi Konno and Masaru Uchiyama (2010). "Vibration Based Control for Flexible Link Manipulator", Robot Manipulators, New Achievements Edited by Aleksandar Lazinica and Hiroyuki Kawai, Tohoku University, Japan, pp. 435-460.
21. Tamer Mansour, Atsushi Konno and Masaru Uchiyama (2011)." Neural Network Based Tuning Algorithm for MPID Control", Industrial Engineering and Management, PID Control, Implementation and Tuning Edited by Dr. Tamer Mansour, Tohoku University Japan, pp. 163-188.
22. Auwalu M. Abdullahi, Z. Mohamed, Mustapha Muhammad and A. A. Bature (2013). "Vibration And Tip Deflection Control of a Single-Link Flexible

Manipulator", International Journal of Instrumentation and Control Systems (IJICS) Vol.3, No.4.

23. Shubham Pareek et. al. (2014). "Optimal Tuning of PID Controller Using Genetic Algorithm and Swarm Techniques", International Journal of Electronic and Electrical Engineering, Volume 7, Number 2, pp. 189-194.
24. G. Madasamy, C. S. Ravichandran (2014). "PID Controller Tuning Optimization with BFO Algorithm in AVR System", International Journal on Recent and Innovation Trends in Computing and Communication (IJRITCC), Volume 2 Issue 12, pp. 3823 – 3827.
25. P. Siva Subramanian and R. Kayalvizhi (2015). "An Optimum Setting of PID Controller for Boost Converter Using Bacterial Foraging Optimization Technique" in Systems Thinking Approach for Social Problems: Proceedings of 37th National Systems Conference, December 2013, V. Vijay, S. K. Yadav, B. Adhikari, H. Seshadri, and D. K. Fulwani, Eds., ed New Delhi: Springer India, pp. 13-23.
26. M.O. Tokhi and A.K.M. Azad (2008). "Flexible Robot Manipulators Modelling, Simulation and Control", The Institution of Engineering and Technology.
27. Mohammad Faisal Hashim, Mohd. Sanawer Alam (2013). "Evaluations of Optimum Value of PID Controller Gains Using Hybrid Bacterial Swarm Optimization", Electronics Instrumentation & Control Engineering, Azad Institute of Engineering & Technology, International Journal of Engineering Research & Technology, ISSN: 2278-0181, Vol. 2 Issue 11.
28. B. Sumanbabu, S. Mishra, B.K. Panigrahi, and G.K. Venayagamoorthy (2007). "Robust Tuning of Modern Power System Stabilizers Using Bacterial Foraging Algorithm", Department of Science and Technology the University of Missouri, Rolla, USA.
29. Ahmed H. Abo absa1, Mohammed A. Alhanjouri (2012). "PID Parameters Optimization Using Bacteria Foraging Algorithm and Particle Swarm Optimization Techniques for Electrohydraulic Servo Control System", The 4th International Engineering Conference –Towards engineering of 21st century.
30. Chen Li (2013). "Application of Bacterial Foraging Optimization PID Control in VAV System", International Conference on Computer Science and Electronics Engineering, China.